Applied Thermal Engineering 35 (2012) 120–126

Contents lists available at SciVerse ScienceDirect

Applied Thermal Engineering

journal homepage: www.elsevier.com/locate/apthermeng

Effects of secondary variables on infiltration rate of open refrigerated vertical display cases with single-band air curtain

Mazyar Amin [a,*], Dana Dabiri [a], Homayun K. Navaz [b]

[a] Aeronautics and Astronautics Department, University of Washington, Seattle, WA 98195, USA
[b] Mechanical Engineering Department, Kettering University, 1700 University Ave., Flint, MI 48504, USA

ARTICLE INFO

Article history:
Received 26 June 2011
Accepted 8 October 2011
Available online 18 October 2011

Keywords:
Infiltration
Entrainment
Air curtain
Open refrigerated display case
Tracer gas

ABSTRACT

Recently the authors of this work reported the effects of several *primary* variables that can affect the performance of a circulated air curtain in protecting open refrigerated vertical display cases against infiltration of outside warm air. Those variables were either associated with the dynamics of the air curtain flow or were geometrical variables. There were a few other variables that were thought to have lesser impact on infiltration or relatively much harder to manage and vary; therefore, they were categorized as, so-called, *secondary* variables and decided to be studied separately in a complimentary investigation. These variables were not included in the permutations of the *primary* variables as they would drastically increase the number of experiments in the published *primary*-variables study. Due to using a few simplified assumptions or ideal conditions in the *primary* study, the *secondary* variables' effects were incorporated as several correction functions to modify the infiltration rate obtained from the *primary* study. The four *secondary* variables studied here are turbulence intensity of the air curtain jet at its discharge nozzle, average percentage of the space between the shelves that was filled with food products, difference between the temperatures of ambient air and the jet at the discharge nozzle, as well as the relative humidity between the aforementioned locations. For the ranges of the variables commonly used in typical medium-temperature display cases, it was found that the temperature and relative humidity changes are of little or no importance, while the turbulence intensity changes infiltration rate almost linearly and the food level varies it in a nonlinear manner.

1. Introduction

Supermarkets significantly contribute to the consumption of electricity. Among those supermarkets that employ open refrigerated vertical display cases (ORVDCs), up to 50% of the cost is attributed to these systems. Also up to 80% [1] of the energy cost of each individual system can be associated with the entrainment and penetration of outside warmer air into the system. Previous studies [2,3] on ORVDCs have indicated that the temperature distribution in the cold storage area is vulnerable to temperature difference between the cold supplied air and ambient air, and will increase with the increase of the latter. This can be more pronounced in non-circulated air curtains such as those used at the entrance of buildings, where, the air curtains may lose relatively more momentum than those of the recirculated ones (such as those in ORVDC's) or may have excessive momentum that causes forceful impingement on the floor. In ORVDCs however, the air curtain regains some momentum near the return passage, which can help the air curtain better retain its integrity. A computational study [4] has demonstrated that in circulated air curtains, when the momentum of the air curtain is not sufficiently low, the infiltration of ambient air into the cold space is not enhanced by an increase of the ambient air temperature. This suggests that the performance of air curtains in insulating one space from the other is not affected by the temperature difference when buoyancy effect is insignificant; however, the amount of the load will be higher when ambient temperature increases. In sufficiently distant locations in the downstream of the air curtain nozzle, the loss of momentum signifies the temperature gradient by creating an additional transverse pressure difference (stack effect) [5,6] that may deform the air curtain stream. Under other circumstances, an adverse upward flow may be produced due to buoyancy effect [6,7]. In an attempt to investigate the thermal effect on the development and performance of air curtains, the effects of Reynolds and Richardson numbers were studied [8]. One interesting finding was that flow

* Corresponding author. Current address: Parks College of Engineering, St. Louis University, 3507 Lindell Blvd, St. Louis, MO 63103, USA. Tel.: +1 (206) 931 7621; fax: +1 (314) 977 8288.
E-mail addresses: mazyar@uw.edu, mamin2@slu.edu (M. Amin), dabiri@aa.washington.edu (D. Dabiri), hnavaz@kettering.edu (H.K. Navaz).

1359-4311/$ – see front matter © 2011 Elsevier Ltd. All rights reserved.
doi:10.1016/j.applthermaleng.2011.10.013

tends to be momentum-driven in air curtains for discharge Reynolds numbers (*Re*) over 100 (note: the cited or used *Re*'s in this work are defined as $\dot{m}_{DAG}/(\mu w_{DAG})$ where $\dot{m}_{DAG}$, μ are, respectively, the mass flow rate and dynamic viscosity of air at the discharge nozzle and w_{DAG} is the width of the discharge nozzle). Since typical ORVDCs operate at Reynolds number between 3000 and 5000, one may conclude that the air curtains of most ORVDCs are momentum-driven. Recently, it was shown [9] that in relatively tall ORVDCs (e.g. $H/w = 16$, H: height of the opening, w: smaller dimension of the air curtain nozzle exit) that have a large horizontal offset distance between the discharge nozzle and return passage the mean streamwise velocity of the air curtain jet at the center point of the discharge nozzle plunges 70% at Reynolds number of 3500. At this point, a maximum drop of approximately 85% is estimated for the mean value of an equivalent nozzle width, bringing about $Re \approx 500$, which is still greater than the critical value of 100. This emphasizes that almost in the entire air curtain path, the thermal effects are minimal; nevertheless, one should not neglect such effects in other regions of the flow domain, in or out of the display cases, where the influence of the air curtain is not significant.

The work of Hayes [10], Hayes and Stoecker [5,11], Hestroni [12], and Hestroni et al. [13], were some of the pioneers in the study of air curtain developments and heat and mass transfer through air curtains. Hayes [10] reported that at turbulence intensity of 8% at the jet exit, a faster rate of spreading of their non-circulated air curtain was observed compared to air curtains with 1% turbulence intensity. The other studies, however, considered a very low turbulence intensity (1% or below). Howell et al. [14], numerically and experimentally studied a non-circulated air curtain as well. They varied their turbulence intensity from 1% to 14% and noticed that the initial region (also called potential region) of the jet significantly and linearly decreases as the turbulence intensity increases. Also Navaz et al. [15] experimentally measured turbulence intensity and noticed that due to the presence of the honeycomb, there is continuous variation in the turbulence intensity across the width of the jet exit. The also incorporated some of the experimental data obtained by PIV and LDV methods into a CFD model and demonstrated that the entrainment rate varies with turbulence intensity especially at higher Reynolds numbers. The variations in the entrainment were mostly linear. However, they did not measure the actual amount of the entrained air that was entrained. Although the infiltration is brought about by entrainment, change in the certain amount of entrained air does not necessitate the same amount of change in the infiltrated air.

The current work is complementary to a previous study [16] that took into account the effects of some key parameters that could impact the infiltration rate in ORVDCs. We focus on those variables that are postulated to have *secondary* effects on infiltration rate.

2. Problem description

In the previous work [16], it was shown that the non-dimensional infiltration rate (*N.I.R.*) in an ORVDC can potentially be a function of several non-dimensional variables presented in Eq. (1):

$$\left(N.I.R. = \frac{\dot{m}_{\inf}}{\dot{m}_{tot}}\right) = \underbrace{f\left(\frac{H}{w}, \alpha, \beta, \mathrm{Re}, \frac{\dot{m}_{BP}}{\dot{m}_{tot}}\right)}_{\text{primary variables function}} \times \underbrace{\Theta\left(\frac{T_{Am} - T_{DAG}}{T_{Am}}\right) \times \Omega(R.H.) \times \Phi(I_{DAG}) \times \Psi(K)}_{\text{secondary variables functions}} \quad (1)$$

In this equation functions f, Θ, Ω, Φ, Ψ relate the above non-dimensional variables to infiltration rate. These functions except f are considered as *correction functions* in this work. The variables are defined below and some of them have been depicted in Fig. 1 as well.

N.I.R.: Non-dimensional infiltration rate

$\dot{m}_{Inf}$: Mass flow rate of infiltrated air

$\dot{m}_{tot}$: Total flow rate of the ORVDC (i.e. flow through the return passage)

H: Opening height

w: Width of the return

α: Offset angle

β: Throw angle

Re: Reynolds number ($= \dot{m}_{DAG}/(\mu w)$) at the air curtain discharge

$\dot{m}_{BP}$: Mass flow rate issued horizontally from the back panel wall

T_{Am}: Ambient temperature

T_{DAG}: Temperature at the air curtain discharge

R.H.: Relative humidity of ambient

I_{DAG}: Turbulence intensity at the air curtain discharge

K: Food level (percentage of the space between the shelves covered with food)

The *primary* variables in Eq. (1) are those believed to have more influence on the amount of infiltration than the other variables (*secondary* variables). Categorizing these variables as *secondary* variables is due to their potentially lesser significance or extreme difficulty in continuously varying or maintaining a variable for the purpose of a parametric study. The effect of the *primary* variables has been previously [16] discussed in detail. In that work, the infiltration experiments were performed for all possible permutations of the *primary* variables, which yielded hundreds of infiltration data points. In the current work, the focus will be on the effect of the *secondary* variables and finding the functions Θ, Ω, Φ, Ψ in Eq. (1). These functions represent correction functions to adjust the function f in Eq. (1) for non-ideal and some other practical conditions. Including the *secondary* variables in studying the combination of all these variables, along with *primary* variables, would increase the number of the tests significantly by a factor of at least $3^4 = 81$ (if each *secondary* variable took at least three values). That means the total number of tests would need to be approximately 46,000.

The *primary* variables were tested under the following conditions:

- No food prototypes on the shelves ($K = 0$)
- Isothermal condition in the entire flow field ($T_{DAG} = T_{Am} = 24\ ^\circ\mathrm{C}$)
- Fixed relative humidity in the entire flow field ($R.H. = 55\%$)
- Relatively low turbulence intensity at the discharge of the air curtain jet ($I_{DAG} = 2.5\% \pm 1\%$).

An *air curtain simulator* (Fig. 2) that was also previously used [16,17] to test the *primary* variables, was utilized to study the effects of various food levels and different turbulence intensity levels. One reason for not considering turbulence intensity as a *primary* variable was that reproducing and attaining the same amount of turbulence intensity repeatedly in different test configurations would be cumbersome. Thus, in the *primary*-variables study, the value of the turbulence was maintained at a relatively low level and was varied in the *secondary*-variable study to achieve higher values. To produce higher turbulence intensities that were uniformly induced everywhere at or before the nozzle exit, loose flappers were utilized that did not affect the mean velocity. As mentioned before, one of the reasons that turbulence intensity was decided to be studied as a *secondary* variable was the difficulty in producing

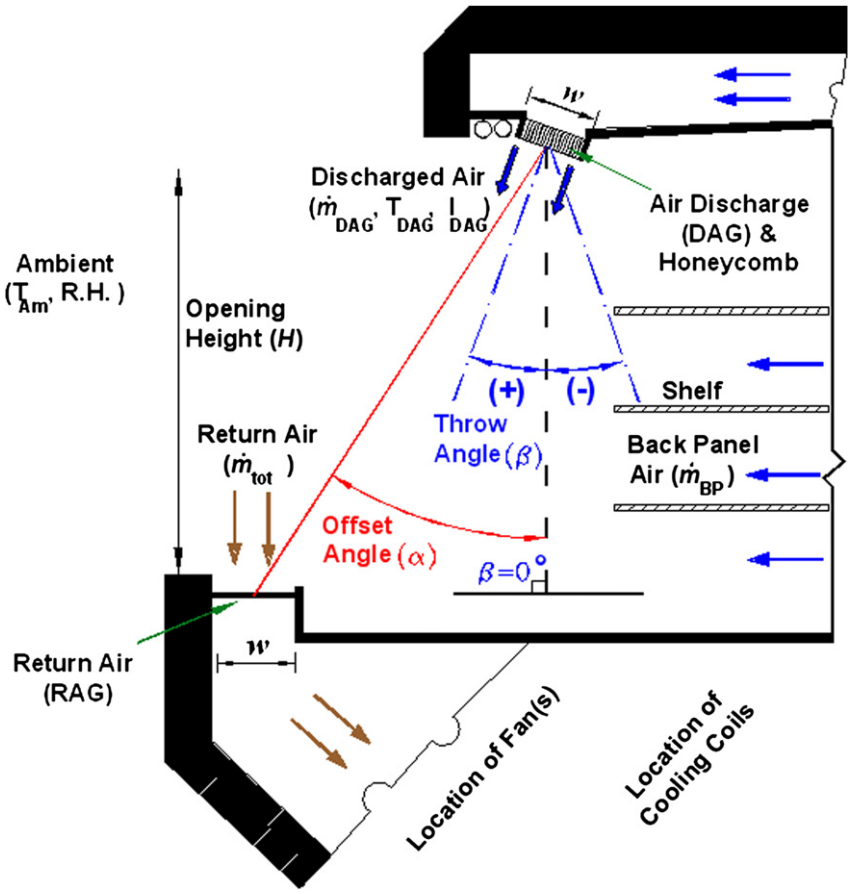

Fig. 1. Schematic of the side view of a section of a typical ORVDC [16].

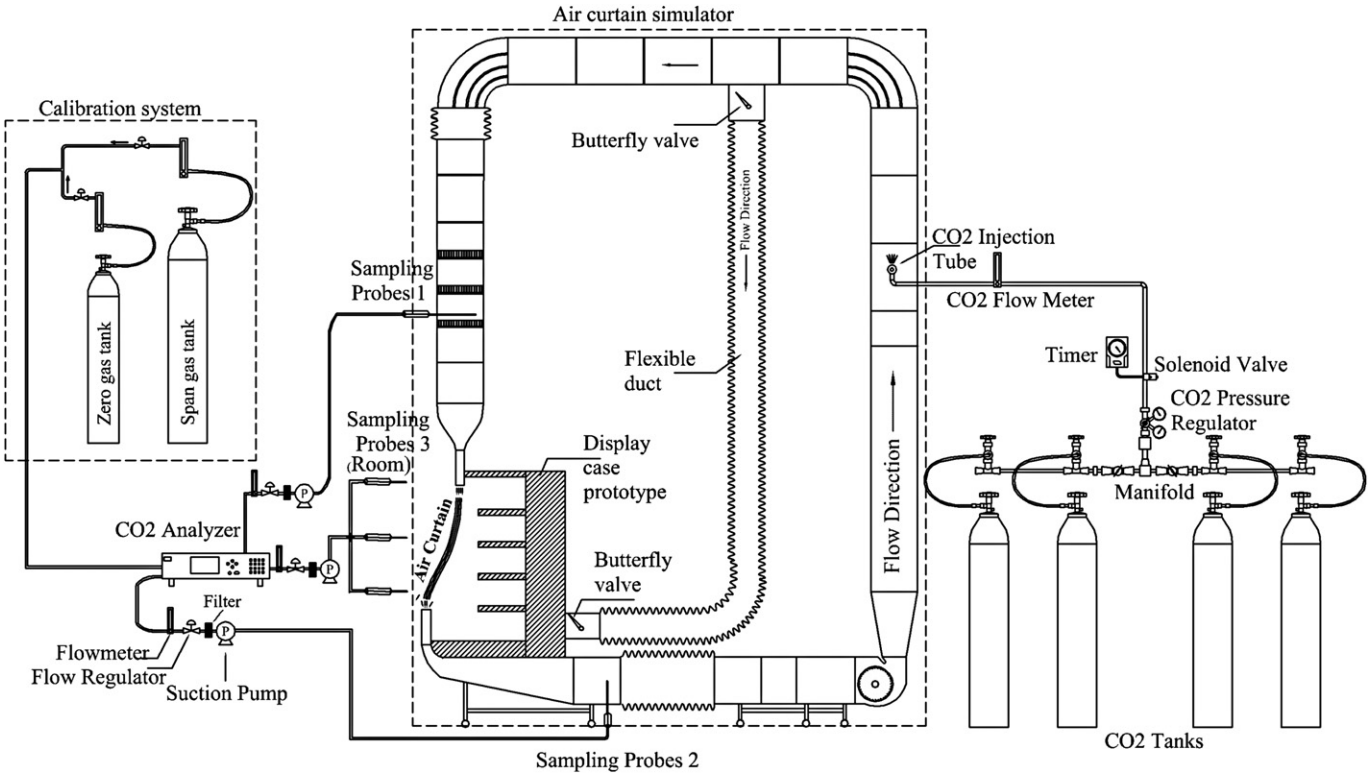

Fig. 2. Air curtain simulator along with infiltration test set up [16].

the same turbulence intensities over and over again for different tests. In our study turbulence was artificially tripped at the upstream of the jet exit. Ironically, adding turbulence to the upstream of our jet exit, where the flow had relatively low agitation, was not very simple. The loose flappers were randomly but evenly placed in the upstream. The amount of those flappers would be changed from one Reynolds number to another in order to create the same intensity for a group of tests. Since this would be very cumbersome to be accomplished for hundreds or thousands of times, it was decided to limit the number of variations for turbulence and include it as a *secondary* variable. The studies on the various temperatures and relative humidity, however, were conducted on a typical ORVDC in the Refrigeration and Thermal Test Center of Southern California Edison Company. The test facility was equipped with an environmentally-controlled laboratory where temperature and relative humidity could be readily controlled.

For the testing, tracer gas method [18] was employed. It was shown that the advantage of this technique over the conventional methods is its higher accuracy that is not compromised, even in the lack of an operating refrigeration system. In addition, the tests can be carried out significantly faster. In our tests, we released carbon dioxide (CO_2) at a location immediately after the fan to enhance the mixing of the gas with air before the mixture was discharged. The concentration of gas was then measured at three regions: 1) in the upstream of the air curtain discharge; 2) in the downstream of the return passage but prior to the releasing site of the gas; and 3) at a close distance across the air curtain. In every region, the samples of air-gas mixture were taken by three separate probes before being merged and transferred to an analyzer of gas concentration (VA-3000, Horiba Co.) by rate of 1 sample/sec. The data were transferred to a computer to calculate the *N.I.R.* using Eq. (2), which was thoroughly discussed in reference [18]:

$$N.I.R. = \frac{\dot{m}_{inf}}{\dot{m}_{tot}} = \frac{C_{Dis} - C_{RAG}}{C_{Dis} - C_{Am}} \tag{2}$$

In this equation C denotes the mass concentration of sampled tracer gas. Indices *Dis*, *RAG* and *Am* represent, respectively, the regions 1 through 3 that were described above. Before the tests were conducted, CFD simulations using a commercial program (Fluent, ANSYS Inc.) were performed [18] to identify the proper locations of the sampling probes that ought to be installed to measure the concentration of gas across the air curtain and inside the room (C_{Am}).

3. Results and discussions

The focus of this section will be on correlating *secondary* variables with infiltration rate as shown in Eq. (1). In order to find this correlation, the infiltration tests were performed for several values of each *secondary* variable. Then the correction functions in Eq. (1) were multiplied by the infiltration obtained from the *primary* variables (i.e. $f(\ldots)$ in the equation. It should be noted that the data points of the *secondary* variables were fewer than those of the *primary* variables, as they were not tested for all possible combinations.

3.1. Effect of food level

The average percentage of the space between the shelves occupied by food is potentially important as the food product can: 1) partially or completely block the flow issued horizontally from the back panel and alter the amount of supplied cold air that is responsible for maintaining a sufficiently low temperature for food products; 2) alter the ratio $R = \dot{m}_{BP}/\dot{m}_{tot}$ and consequently the overall dynamics of the cross flow (flow–flow interaction of the vertical air curtain flow with horizontal back panel flow); and 3) change the dynamics of the air curtain flow by changing its flow-structure interaction (discussed in the following). In order to comprehend the effect of food level, infiltration tests were performed at different Reynolds numbers (3 levels), α (2 levels: 0°, 24°), and R (2 levels: 0% and 55%). Angle β and H/w were maintained at 0° and 12, respectively. The tests were performed at three food levels of 0%, 35%, and 80%.

Although Fig. 3 indicates the infiltration value depends on geometrical configurations and R, at a fixed geometrical configuration, variation of Reynolds number results in very similar infiltration rate trends. The infiltration either decreases monotonically with increase of food level (Fig. 3 (X*a,d*)), or first experiences an uphill and then plummets (Fig. 3 (X*b,c*)). It seems that in the latter cases, the maximum *N.I.R.* occurs at food levels around 30%, while in all cases the smallest infiltration rate takes place at the highest food level (i.e. 80%). This minimum infiltration perhaps happens because when the vertical space between the shelves is filled with more food products, the periodic configuration of the shelves that usually intervenes with flow in the form of perpendicular impingement, resembles more a flat vertical surface from which the turbulence will not be induced or enhanced due to elimination of direct impingement. Therefore, there are two extremes for the flow-structure interaction, ranging from direct perpendicular impingement on the shelves to passing by the shelves parallel to the vertical edge of the food products and creating almost a boundary layer. One can observe in some cases that the infiltration may not drop, but may even increase when food level increases from low to medium. This may be an indication of strong impingements that can still exist in those cases.

Comparing the *N.I.R.*s at offset angles 0° and 24° suggests that the order of change of *N.I.R.* with respect to *Re* also depends on the value of offset angle. For example at $\alpha = 0°$, $Re = 8400$ results in the smallest *N.I.R.* among other *Re* values, while it produces the largest infiltration for $\alpha = 24°$. In an experimental study that visualized (by particle image velocimetry) the flow in a cavity insulated by a similar air curtain, it was shown that [9] at medium H/w values (e.g. $H/w = 12$), there is higher chance that the air curtain impinges forcefully on the lowest horizontal surface (tray) of the display case. By comparing these two studies one can infer that at greater offset angles, after passing the shelves area (whether or not partially impinging on them) the air curtain will hit the bottom surface with higher momentum than those air curtains with lower Reynolds number. After the strong impingement at higher Reynolds numbers, an upward flow will be created that will in turn induce more agitation to the flow and will give rise to higher levels of turbulent kinetic energy and associated turbulent shear stress in that region. Therefore, the vortices that are created in the lower part of the display case as a result of such agitations can bring about more entrainment of outside warmer air (by air curtain) that will consequently enhance the possibility of infiltration.

As appeared in Eq. (1), Ψ, is a correction function corresponding to the effect of food level and is interpreted as a *normalized non-dimensional infiltration rate,* i.e., it is an *N.I.R.* normalized by the value of *N.I.R.* at 0% food level (called $N.I.R_{no,food}$):

$$\Psi(K) = \frac{N.I.R.}{N.I.R._{no,food}} \tag{3}$$

To take into account the effect of food level, this function modifies the values of infiltration for the cases with zero food level. It was found that at $R = 0$, averaging the results over the values of different Reynolds numbers would result in:

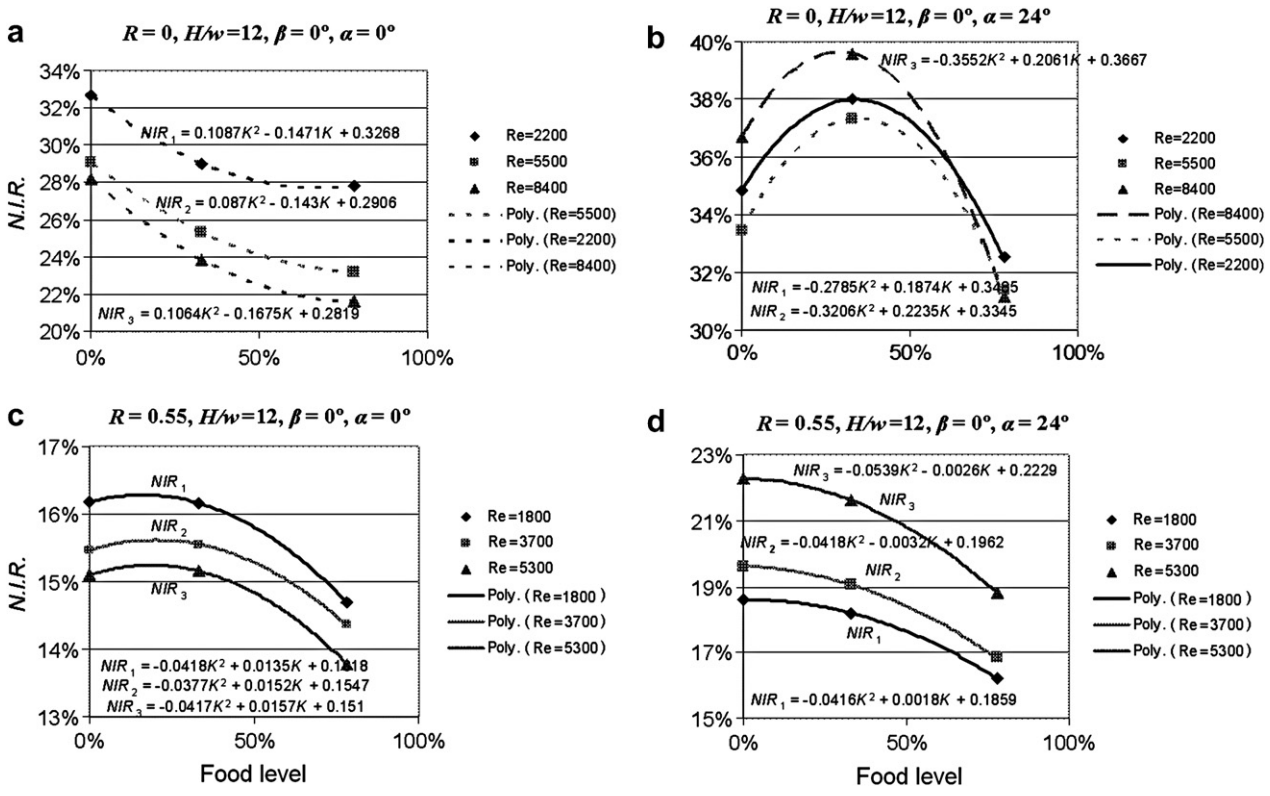

Fig. 3. Dependency of *N.I.R.* on food level.

$$\Psi_1 = \frac{\alpha}{24}\left(-1.27K^2 + 1.11K\right) + 0.362K^2 - 0.52K + 1 \quad (4)$$

and in the same fashion at $R = 0.55$:

$$\Psi_2 = \frac{\alpha}{24}\left(-0.033K^2 - 0.646K\right) - 0.259K^2 + 0.64K + 1 \quad (5)$$

With linear interpolation between Eq. (4) and (5) (with respect to R) one can estimate an overall correction function:

$$\Psi = 0.55(1 - R)[\Psi_2 - \Psi_1] + \Psi_1 \quad (6)$$

Ψ, Ψ_1, Ψ_2 are functions of K, α and R. Hence, the corrected infiltrations can be expressed as:

$$(N.I.R.)_{with_food} = (N.I.R.)_{no_food} \times \Psi \quad (7)$$

3.2. Effect of temperature difference

Further investigations were conducted to find the effect of differences between the temperature of the discharged air curtain and ambient temperature ($\Delta T = |T_{Am} - T_{DAG}|$) on the infiltration rate. Tests were performed at medium refrigeration temperatures i.e. $-3\,^{\circ}C < T_{DAG} < 2\,^{\circ}C$ in an environmentally-controlled laboratory of Southern California Edison Company. The results indicate that at a fixed ambient temperature (T_{Am}), infiltration is a weak function of the discharge air temperature, T_{DAG}, for typical vertical display cases with $Re = [3000\ 5000]$. In the laboratory the ambient temperature and relative humidity were kept constant at 24 °C and 55%, respectively. Also, all tests were performed within 30 min after defrost of the refrigeration cycle to ensure that the air flow rate is consistent for different tests. The results have been summarized in Table 1. In these tests, the average value of *N.I.R.* was 28.4% with a standard deviation of only 0.26%. The uncertainty associated with this measurement technique is about 3% of the full scale. Therefore, the standard deviation in Table 1 falls within the range of the testing uncertainty.

It can be expected, however, that under some conditions (outside of the scope of current study) when the overall momentum of the flow gets smaller than the critical value discussed before, temperature difference plays a more important role on infiltration, and the buoyancy and stack effect [5] get pronounced and dominate the momentum of the air curtain flow. For example, if the air curtain flow rate drops significantly, diffusion rises compared to convection, and therefore the buoyancy effect ought to be taken into consideration [8]. Previous studies [4] verify the small effect of the above temperature difference on infiltration. However, it should be noted that this does not mean the cooling load of the refrigeration system is independent of ΔT, but emphasizes on this fact that the performance and fluid dynamics of the air curtain is not affected by the difference, at least in the range of typical operating temperatures and Reynolds numbers. For example, the amount of sensible load of the system, i.e. $\dot{Q} = \dot{m}C_p\Delta T$, is not affected, as this study shows, by the mass flow rate of the infiltrated air $\dot{m}$ (when ΔT increases), but the load obviously increases with increase of ΔT.

Therefore, in the above range of operation, the temperature correction function Θ in Eq. (1) will become almost constant and independent of ΔT. We set $\Theta \approx 1$, as almost no correction is required for infiltration in this regard.

Table 1
Dependency of non-dimensional infiltration rate on discharge air temperature.

T_{DAG} (°C)	−3	0	2	Average	Standard deviation
N.I.R. (%)	28.2	28.3	28.7	28.4	0.26

3.3. Effect of relative humidity

The investigation on the effect of ambient relative humidity (*R.H.*) was conducted in the same laboratory. In a series of experiments, the *R.H.* was changed from 30% to 65% and its effect on infiltration rate was measured at a fixed ambient temperature of 24 °C and discharge air temperature of 0 °C (Table 2). In these tests, the average value of *N.I.R.* was 33.6% with a standard deviation of 0.67%. The standard deviation falls within the range of the testing uncertainty. From the result of Table 2 it is evident that similar to the effect of ΔT discussed previously, the variation of the *R.H.* does not have significant effect on the amount of infiltration either. Overall, one can conclude that the correction function for relative humidity to be approximated $\Omega \approx 1$. It should be noted that in this table, the values of non-dimensional infiltration are somewhat larger than those in Table 1 for the counterpart values of temperature and humidity. The difference is due to the fact that after testing the temperature effect, the display case was partially retrofitted. However, regardless of the geometrical configuration of the system, one can draw useful comparative and qualitative conclusions as all the tests on the effect of relative humidity were performed in the same geometrical and fluid conditions.

An interesting conclusion from the above experiments yielding small variations of infiltration with change of ΔT and *R.H.*, is that our simulator system, which lacks a refrigeration system, provides us with reasonable infiltration results. This infers that it is not necessarily required to have a refrigeration system to measure the infiltration by traditional methods, i.e. collection of the condensate mass of the refrigeration system and relating that to the outside infiltrated air [19,20], or using a *thermal entrainment* equation [21]:

$$\left|\frac{T_{DAG} - T_{RAG}}{T_{DAG} - T_{Am}}\right| \tag{8}$$

The traditional methods are obtained from conservation of energy in and around the system, while in tracer gas method conservation of mass is utilized [18].

3.4. Effect of turbulence intensity at discharge of nozzle

In this work, turbulence intensity at the discharge of the nozzle is defined as $u\prime/U$, where u' is the root mean square (rms) value of velocity fluctuations, and U is the mean velocity of the flow. Because the turbulence intensity of the jets exiting the nozzle (I_{DAG}) of our air curtain simulator varies between 1.5% and 3.5%, and the turbulence intensities of typical ORVDC's varies between 10% and 20%, we attempted to add artificial agitation to the flow at the upstream of the nozzle exit and also at the exit of the nozzle to induce more turbulence. To achieve this, flow obstructions such as flappers were installed before the discharge, where the turbulence intensity was incrementally increased up to 13%. Tests were done for empty, as well as, partially filled shelves. As one may expect, our results indicated that an increase of turbulence intensity enhances the amount of infiltration. It was also found that in the range that the variables change in the current work, infiltration and turbulence intensity are almost linearly related (Fig. 4). From there, the turbulence intensity (I_{DAG}) correction function Φ in Eq. (1) can be derived as:

Table 2
Dependency of non-dimensional infiltration rate on ambient relative humidity.

Ambient *R.H.* (%)	30	45	55	65	Average	Standard deviation
Non-dimensional infiltration rate (%)	34.4	33	33.1	33.9	33.6	0.67

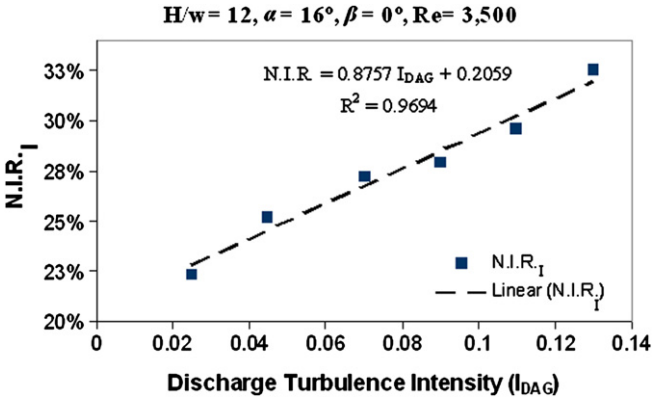

Fig. 4. Variation of *N.I.R.* with turbulence intensity at the jet exit at $K = 60\%$.

$$\Phi(I_{DAG}) = \frac{N.I.R._I}{N.I.R._{\circ,I}} = 1 + \frac{E}{N.I.R._{\circ,I}} \tag{9}$$

where $N.I.R._I$ is the value of the non-dimensional infiltration rate when the jet exits with an artificially added turbulence. $N.I.R._{o,I}$ corresponds to the non-dimensional infiltration rate before adding the turbulence (i.e. at I_{DAG} 2.5% ± 1%).

The parameter E was found to be:

$$E = 0.876 \times I_{DAG} - 0.022 \tag{10}$$

Consistent with this finding, Howell et al. [14] showed that the length of potential core of a jet decreases almost linearly as the turbulence intensity increases. This infers that with increase of turbulence intensity, the mixing at the outer edges of the jet develops more rapidly and the effect of shear will penetrate towards the center of the jet at a faster pace. As a result of the mixing, more flow from ambient can be entrained by the jet.

4. Conclusions

It has been shown that infiltration is a weak function of the variables associated with the thermal energy content of air (i.e. temperature difference and relative humidity). In this regard, the variation of discharged air temperature at a constant ambient temperature does not affect infiltration, implying that for air curtains with typical Reynolds numbers, the momentum of flow and heat convection predominate the mass and heat diffusion due to temperature difference. These findings confirm that our infiltration tests that were performed with a lack of refrigeration system were valid. The observations, nonetheless, do not infer that the total cooling load of the refrigeration system is independent of temperatures; conversely, it is evident that with an increase of ambient temperature and humidity, or an increase of the discharge temperature, the load increases as well.

In most cases, high food level lowers the infiltration rate by providing a virtual, quasi-flat wall boundary at the tip of the shelves that helps attenuates the nearly perpendicular impingement of the jet on the shelves. On the other hand, an excessive increase of the food level may not be recommended as it may limit the amount of transverse cold air that should flow over the shelves and food products to maintain their temperature sufficiently low. Also, the higher the turbulence intensity of flow at the exit of the air curtain nozzle, the higher infiltration will be brought about. The relation between the turbulence intensity and infiltration was found to be almost linear.

With the correction functions found in this work, the infiltration of ambient air into the return passage can be predicted more

accurately by modifying the infiltration rates measured from the study of the *primary* variables [16]. The corrected infiltrations will help the designers and manufacturers of open refrigerated display cases design more energy-efficient systems that can be achieved by making minor changes, saving U.S. supermarkets upwards of millions of dollars per year. Based on an estimation by the California Energy Commission, the energy savings associated with a 15% reduction in the energy consumption in open refrigerated display cases would be about $100 million dollars per year in the United States. This estimation, however, is based upon the electricity prices of 1999. With the current higher rates, our success in achieving more efficient systems (at least 25% reduction), and current bigger market for such systems, the figure for the savings is expected to be significantly higher.

Acknowledgements

This work was sponsored in part by the U.S. Department of Energy (under contract DE-AC05-00OR22725 with UTBattelle, LLC.), California Energy Commission and Southern California Edison Company.

References

[1] R.H. Howell, P. Adams, Effects of Indoor Space Conditions on Refrigerated Display Case Performance. ASHRAE, 1991.
[2] Y.G. Chen, X.L. Yuan, Simulation of a cavity insulated by a vertical single band cold air curtain, Energy Conversion and Management 46 (2005) 1745–1756.
[3] Y.T. Ge, S.A. Tassou, Simulation of the performance of single jet air curtains for vertical refrigerated display cabinets, Applied Thermal Engineering 21 (2001) 201–219.
[4] H.K. Navaz, R. Fararmarzi, D. Dabiri, M. Gharib, D. Modarress, The application of advanced methods in analyzing the performance of the air curtain in a refrigerated display case, Journal of Fluid Engineering 124 (2002) 756–764.
[5] F.C. Hayes, W.F. Stockers, Design data for air curtains, ASHRAE Transactions (1969) 153–167.
[6] Y.G. Chen, Parametric evaluation of refrigerated air curtains for thermal insulation, International Journal of Thermal Sciences 48 (2009) 1988–1996.
[7] G. Cortella, CFD-aided retail cabinets design, Computers and Electronics in Agriculture 34 (2002) 43–66.
[8] B. Field, R. Kalluri, E. Loth, PIV Investigation of Air-Curtain Entrainment in Open Display Cases (2002).
[9] M. Amin, Aerodynamics of air curtains passing over a cavity with a downstream sink, Ph.D. dissertation, Aeronautics & Astronautics Dept., University of Washington, (2010).
[10] F.C. Hayes, Heat transfer characteristics of the air curtain: a plane jet subjected to transverse pressure and temperature gradient, PhD dissertation, University of Illinois, IL (1968).
[11] F.C. Hayes, W.F. Stockers, Heat transfer characteristics of air curtain, ASHRAE Transactions (1969).
[12] G. Hestroni, Heat transfer through and air curtain, PhD dissertation, Michigan State University (1963).
[13] G. Hestroni, C.W. Hall, A.M. Dhanak, Heat transfer properties of an air curtain, ASAE Transactions (1963) 328–334.
[14] R.H. Howell, N.Q. Van, C.E. Smith, Heat and moisture transfer through turbulent recirculated plane air curtains, ASHRAE Transactions 82 (1976) 191–205.
[15] H.K. Navaz, B.S. Henderson, R. Fararmarzi, A. Pourmovahed, F. Taugwalder, Jet entrainment rate in air curtain of open refrigerated display cases, International Journal of Refrigeration 28 (2005) 267–275.
[16] M. Amin, D. Dabiri, H.K. Navaz, Comprehensive study on the effects of fluid dynamics of air curtain and geometry, on infiltration rate of open refrigerated cavities, Applied Thermal Engineering 31 (2011) 3055–3065.
[17] M. Amin, D. Dabiri, H.K. Navaz, Air curtain performance studies in open vertical refrigerated display cases, in: Heat Transfer 2008 Conference, Slovenia (2008).
[18] M. Amin, D. Dabiri, H.K. Navaz, Tracer gas technique: a new approach for steady state infiltration rate measurement of open refrigerated display cases, Journal of Food Engineering 92 (2009) 172–181.
[19] R. Fararmarzi, M. Amin, H.K. Navaz, D. Dabiri, D. Rauss, R. Sarhadian, Air Curtain Stability and Effectiveness in Open Vertical Refrigerated Display Cases (2008) Report prepared for the California Energy Comission, Contract No. CEC-500-05-012.
[20] H.K. Navaz, R. Fararmarzi, Advanced Supermarket Display Case Workshop. ASHRAE, 2004, Winter Meeting.
[21] G. Rigot, Meubles et vitrines frigorifiques pour la distribution alimentaire, first ed. Editions Pyc Livers, Paris, 1990.